Biophysical Chemistry 152 (2010) 128–138

Contents lists available at ScienceDirect

Biophysical Chemistry

journal homepage: http://www.elsevier.com/locate/biophyschem

Thermal stability of extracellular hemoglobin of *Glossoscolex paulistus*: Determination of activation parameters by optical spectroscopic and differential scanning calorimetric studies

Patrícia S. Santiago [a], José Wilson P. Carvalho [a], Marco M. Domingues [b], Nuno C. Santos [b], Marcel Tabak [a,*]

[a] Instituto de Química de São Carlos, Universidade de São Paulo, SP, Brazil
[b] Instituto de Medicina Molecular, Faculdade de Medicina da Universidade de Lisboa, Portugal

ARTICLE INFO

Article history:
Received 13 May 2010
Received in revised form 24 August 2010
Accepted 31 August 2010
Available online 7 September 2010

Keywords:
Extracellular hemoglobin
Oligomeric dissociation
Thermal stability
Protein denaturation
DLS
DSC

ABSTRACT

Glossoscolex paulistus hemoglobin (HbGp) was studied by dynamic light scattering (DLS), optical absorption spectroscopy (UV–VIS) and differential scanning calorimetry (DSC). At pH 7.0, cyanomet-HbGp is very stable, no oligomeric dissociation is observed, while denaturation occurs at 56 °C, 4 °C higher as compared to oxy-HbGp. The oligomeric dissociation of HbGp occurs simultaneously with some protein aggregation. Kinetic studies for oxy-HbGp using UV–VIS and DLS allowed to obtain activation energy (E_a) values of 278–262 kJ/mol (DLS) and 333 kJ/mol (UV–VIS). Complimentary DSC studies indicate that the denaturation is irreversible, giving endotherms strongly dependent upon the heating scan rates, suggesting a kinetically controlled process. Dependence on protein concentration suggests that the two components in the endotherms are due to oligomeric dissociation effect upon denaturation. Activation energies are in the range 200–560 kJ/mol. The mid-point transition temperatures were in the range 50–65 °C. Cyanomet-HbGp shows higher mid-point temperatures as well as activation energies, consistent with its higher stability. DSC data are reported for the first time for an extracellular hemoglobin.

1. Introduction

The giant extracellular hemoglobin of *Glossoscolex paulistus* (HbGp) is characterized by a molecular mass of 3.6×10^6 Da [1], being constituted by a large number of subunits containing the heme group, with molecular masses in the range 15–19 kDa. These heme-containing subunits form monomers of 16 kDa (*d*) and heterotrimers of 51–52 kDa (*abc*), linked by nonheme structures (24–32 kDa) named linkers [2–5]. A recent partial characterization of molecular mass of HbGp [5] confirmed the similarity of its subunits to those of homologous proteins of this class [2–4,6]. This characteristic multi-subunit content confers on the whole protein a double-layered hexagonal oligomeric structure [3,7]. It is worthy of notice that HbGp belongs to the same class of hemoglobins as the hemoglobin of *Lumbricus terrestris* (HbLt), one of the most studied hemoglobins in this group [8–10]. Due to its extracellular nature, large size and resistance to oxidation, giant extracellular hemoglobins, also known as erythrocruorins, have been proposed as useful model systems for developing therapeutic extracellular blood substitutes [6]. Since cell membranes are not present and the protein is not glycosilated, hexagonal bilayer hemoglobins are easy to store, their side effects are less pronounced, and they are less likely to trigger immunogenic responses [6].

In this paper, we report on the thermostability of two different iron oxidation forms of HbGp: the reduced and functional oxy-HbGp, and the oxidized cyanomet-HbGp. In a previous work, we used dynamic light scattering (DLS) to monitor changes in molecular size of oxy-HbGp upon temperature-induced denaturation and dissociation [11]. Kinetic studies of oligomeric dissociation were also performed at alkaline pH and at a fixed temperature of 25 °C. In that paper, a model was proposed for HbGp oligomeric dissociation, based on the expected species present in equilibrium in solution, as a function of the alkalization of the medium. At pH 7.0 a high thermal stability was observed for the oxy-HbGp and a change of size was detected at a critical temperature, implying some protein aggregation induced by high temperatures. UV–VIS spectroscopic kinetic studies were also performed to monitor the auto-oxidation of the protein as a function of pH.

In the present work, further studies were performed with oxy-HbGp, aiming at obtaining the activation parameters related to the dissociation/denaturation process, as monitored by DLS, UV–VIS and also differential scanning calorimetry (DSC). To the best of our knowledge, no information or studies regarding DSC of extracellular hemoglobins exist in the literature. Some interesting research concerning a megadalton oligomeric protein with common features to HbGp is that reporting thermal behavior of hemocyanins [12]. Some

* Corresponding author. Tel.: +55 16 33739979; fax: +55 16 33739982.
E-mail address: marcel@sc.usp.br (M. Tabak).

0301-4622/$ – see front matter © 2010 Elsevier B.V. All rights reserved.
doi:10.1016/j.bpc.2010.08.010

of our present results suggest the existence of similarities between both proteins.

DSC is widely used to determine the thermodynamics of phase transitions and conformational changes in proteins. Equilibrium analysis of DSC thermograms corresponding to reversible unfolding of proteins provides information about the thermodynamics and mechanisms of the reversible unfolding. The thermal denaturation of the hemocyanin from the gastropod *Rapana thomasiana* (RtH) was studied by DSC [12]. A kinetic model for the irreversible denaturation was applied to analyze heat capacity curves that are dependent on the DSC scan rate. Thus, information on the structure in solution and the stability of this respiratory protein was obtained.

Research on the thermal aggregation of globular oligomeric proteins have also been developed based on DLS [13], where the size of the protein aggregates and its evolution with time have been determined [13,14]. These studies were focused on chaperone-like effects of relatively small globular proteins. The DLS data show that the initial stage of thermal aggregation of proteins is the formation of the initial aggregates, involving up to hundreds of molecules of the denatured protein. Further growth of protein aggregates takes place as a result of the sticking of the starting aggregates or the aggregates of higher order.

In our present kinetic studies regarding HbGp thermal stability, besides the partial dissociation of the HbGp as a function of time, and at higher temperatures, some thermal aggregation was also observed. Our main focus is on the oligomeric dissociation observed by DLS and on the denaturation monitored by DSC. Some very preliminary studies regarding aggregation of HbGp in the oxy- and cyanomet-forms are also reported.

2. Materials and methods

2.1. Purification and preparation of HbGp

The hemoglobin of *Glossoscolex paulistus* was prepared using freshly drawn blood from the worms as described earlier [11,15,16]. The blood sample was centrifuged at 4 °C (2300×*g* for 15 min) to eliminate cell debris. An ultra-filtration (molecular mass cut-off 30 kDa) in 0.1 M Tris–HCl buffer pH 7.0, at 4 °C, was performed in order to eliminate low M_w components. After the ultracentrifugation at 250,000×*g*, at 4 °C, during 3 h, HbGp is obtained as a pellet and then resuspended in a minimum amount of 0.1 M Tris–HCl buffer pH 7.0 and stored in the oxy-form at 4 °C. Chromatography at pH 7.0 in a Sephadex G-200 column furnished the samples used in our experiments. All concentrations were determined spectrophotometrically in a Hitachi U2000 spectrophotometer, using the molar extinction coefficients $\varepsilon_{415nm} = 5.5 \pm 0.8$ $(mg/ml)^{-1}\,cm^{-1}$ for oxy-HbGp, and $\varepsilon_{420nm} = 4.8 \pm 0.5$ $(mg/ml)^{-1}\,cm^{-1}$ for cyanomet-HbGp [11,17].

2.2. Dynamic light scattering studies

The commercial instrument Zetasizer Nano ZS (Malvern, UK) was used on the light scattering measurements for particle size determination. This instrument allows dynamic light scattering measurements incorporating noninvasive backscattering (NIBS) optics. A He–Ne laser has been used as a light source with wavelength $\lambda = 633$ nm. The intensity of light scattered at an angle of 173° is measured by an avalanche photodiode. The solutions were placed in the thermostated sample chamber that is temperature regulated for measurements over an interval including the 25–70 °C range, controlled with an accuracy of 0.1 °C. At each temperature seven measurements are performed and for each one a number of measurements is taken (normally around ten) to obtain an adequate statistics. Therefore, each of the seven measurements is an average of around 10 data points. The instrument measures the time dependent fluctuation in intensity of light scattered from the particles in solution. Malvern's DTS software analyses the acquired correlogram (correlation function *vs.* time plot) for the calculation of the hydrodynamic diameter, D_h. Hydrodynamic diameters of the particles were estimated from the autocorrelation function, using the Cumulants method based on a single exponential fit of the correlation function to obtain the mean size (Z-average diameter) and an estimate of the width of the distribution (polydispersity index — PDI). Moreover, an alternative analysis based on a multiple exponential fit of the correlation function, giving the distribution of particle sizes and their contributions to the overall scattering intensity (non-negative least squares – NNLS – or CONTIN), is also performed [18]. The average diffusion coefficient (D) can be calculated from the Stokes–Einstein equation:

$$D = \frac{kT}{3\pi\eta D_h} \tag{1}$$

where k is Boltzmann's constant, T is the absolute temperature and η is the shear viscosity of the solvent.

2.3. Determination of rate constants using DLS measurements

We recently proposed a model characterizing the alkaline dissociation of the dodecamer into the tetramer, followed by dissociation of the tetramer into trimer and monomer [11]. Based on this model, an overall equation for the kinetics of the dissociation was deduced to fit the experimental data of average diffusion coefficient, D_Z, as a function of time:

$$D_Z = \frac{\left(M_p^2 D_p - BD_\infty\right)e^{-kt} + BD_\infty}{\left(M_p^2 - B\right)e^{-kt} + B}. \tag{2}$$

The derivation of this equation is presented in [11]. D_p corresponds to the integer HbGp protein diffusion coefficient; M_p refers to molecular mass of the HbGp; assuming the dissociation of each integer protein into 36 *abc* trimers, 36 *d* monomers and 36 *L* linkers, the parameter B is defined as $B = 36(M_{abc}^2 + M_d^2 + M_L^2)$; D_∞ corresponds to the limiting value of the average diffusion coefficient.

2.4. Auto-oxidation rate measurements

To obtain the rate constants of HbGp auto-oxidation, the absorbance at 415 nm (A_{415}) was monitored over time. The protein concentration was 0.5 mg/ml, the same as for DLS and DSC studies. The oxy-HbGp was monitored from the characteristic relative intensities for the Q-bands. The collected data were fitted to a first-order kinetics as described in [11,19]:

$$A_t = \Delta A_{max} \exp\left(-k_{obs} t\right) + A_\infty \tag{3}$$

In this equation, A_t is the absorbance at time t, A_∞ the absorbance at infinite time, k_{obs} the first-order rate constant, and ΔA_{max} the variation of absorbance ($A_{t=0} - A_\infty$), which corresponds to the total oxidation of the hemes. In general, the auto-oxidation of the native hemoglobin, depending on the solution pH and temperature, requires either the combination of two exponentials or a mono-exponential fit [19]. In the present work only mono-exponential decays were obtained. Three independent experiments were carried out for each condition, and the mean values of the fitted constants are presented.

2.5. Calorimetric studies

Thermal denaturation of HbGp was studied by differential scanning calorimetry. DSC measurements were performed using a VP-DSC, calorimeter, with 0.5 ml sample and reference cells, from MicroCal, LLC (Northampton, MA). The instrumental baseline was determined before each sample scan, by filling both sample and reference cells with the buffer used for the protein samples, and using

the same scanning parameters. All measurements were carried out in 20 mM phosphate–borate buffer at appropriate pH. The protein solution was heated at a rate in the range from 0.5 to 1.5 °C/min, from 20 to 80 °C, at a constant pressure of 2 atm. The reversibility of the thermal transition of HbGp was tested by checking the reproducibility of the calorimetric trace during the second heating of the sample after cooling it back to 20 °C. Before the start, and between repeated heating cycles, the samples were allowed to equilibrate for 30 min at 20 °C.

Heat capacity data were corrected for the instrument baseline, and normalized for scan rate and protein concentration. The protein concentration of the sample in the DSC cell was determined from the absorbance obtained by an independent sample, which was taken as part of the volume of the sample used for DSC, prior to the initial heating cycle. Excess heat capacity profiles were analyzed by using the Origin software provided with the instrument. A progress baseline was fitted to each profile and subtracted, by selecting appropriate pre- and post-transitional segments. The number of components present in the unfolding endotherm and the transition temperature (T_m) were estimated in each case by fitting the thermogram with components corresponding to independent two-state transitions. The number of components in the fitting procedure was kept at the minimum possible that resulted in a good fit to the data. This analysis is similar to that reported in the work of Fodor et al. for Na,K-ATPase [20]. The transition temperatures T_m and the scan rates were used to present the data as Arrhenius plots corresponding to the rate-limiting step of irreversible diffusion-controlled denaturation of HbGp, as described in references [21,22].

3. Results and discussion

3.1. Dynamic light scattering (DLS)

The particle hydrodynamic diameter (D_h) was determined by dynamic light scattering. For cyanomet-HbGp, at 25 °C, in the pH range between 7.0 and 9.8, the protein is in its native oligomeric form, showing a significant stability. The Z-average diameter, followed during 20 h, was 27 ± 1 nm at 25 °C and pH 7.0 (Fig. 1A). At pH 9.0, a slight reduction of diameter is observed to 26 ± 1 nm. Finally, at pH 9.8, a further reduction is observed to an initial diameter of 24 ± 1 nm, which undergoes a very slight increase over time, reaching a value of 25 ± 1 nm during a 20 h monitoring interval. Therefore, for the cyanomet-HbGp (Fig. 1A) solutions, changes in pH on the 7.0–9.8 range, at 25 °C, did not exert such a dramatic particle diameter alteration as observed previously for oxy-HbGp [11], suggesting that the degree of aggregation and macromolecule stability, at room temperature, remain the same independent of pH. Fig. 1B shows the corresponding particle size distributions from the DLS data of cyanomet-HbGp presented in Fig. 1A. The average polydispersion indexes at pH values 7.0, 9.0 and 9.8 are 0.01, 0.08 and 0.14, respectively. In our previous work we associated the increase of polydispersion indexes with the phenomenon of the dissociation of oxy-HbGp [11]. For cyanomet-HbGp, the increase of polydispersion indexes could be associated with partial dissociation or loosening of the protein structure at alkaline pH. At pH higher than 9.0, for oxy-HbGp, this process results in the appearance in solution of several dissociation species, such as the dodecamer, tetramer, trimer, linker and monomer, besides the remaining non-dissociated protein in its original form. In the case of cyanomet-HbGp, at 25 °C, no evidence of these lower molecular weight subunits is observed from our DLS data. The slight D_h decrease with the increase of the pH value may be due to the increase of dimensions uncertainties upon increase of the polydispersity (Fig. 1B).

Fig. 2 shows the "melting curves" reporting the variation of D_h as a function of temperature for cyanomet-HbGp at different pH values. It can be seen that in the pH range 7.0–9.0, the increase in temperature induces HbGp partial dissociation before the denaturation. At pH 7.0,

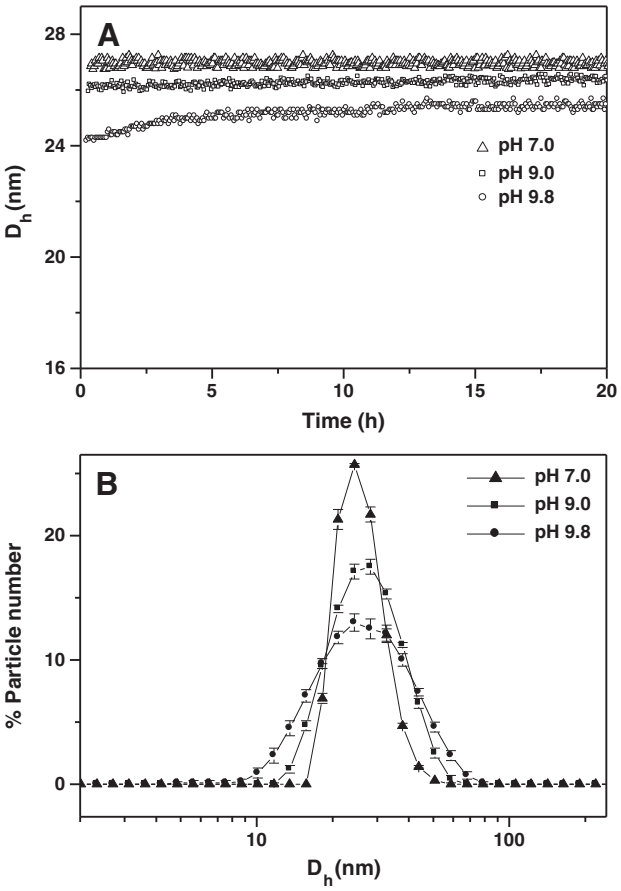

Fig. 1. (A) Variation of the hydrodynamic diameter (D_h) as a function of time for cyanomet-HbGp 0.5 mg/ml at pH values 7.0, 9.0 and 9.8, in acetate–phosphate–borate 30 mM buffer at 25 °C. (B) Particle size distribution from DLS data of cyanomet-HbGp obtained from data similar to that shown in Fig. 1A using the CONTIN method. Error bars represent the standard deviations of fifteen different measures per data point. The time interval corresponds to the first 2 h of the kinetics measurement.

where cyanomet-HbGp is very stable, the temperature does not induce the dissociation of the protein. However, when a high temperature is reached (56 °C) protein denaturation occurs, followed by some protein aggregation, as judged by the formation of a complex with a Z-average D_h of 100 nm (Table 1). As mentioned above, a critical denaturation

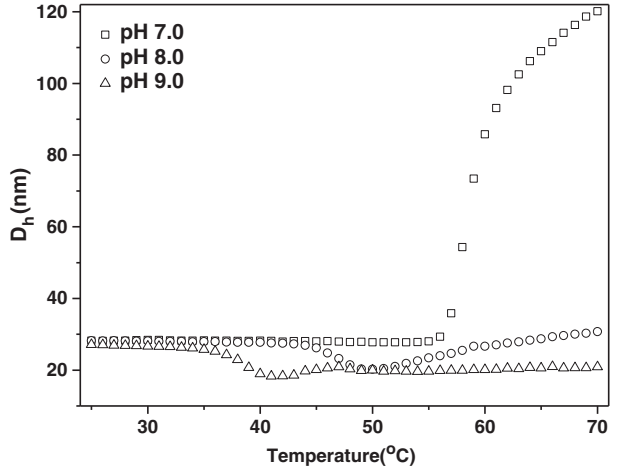

Fig. 2. Effect of temperature on the cyanomet-HbGp hydrodynamic radius at different pH values. [HbGp] = 0.5 mg/ml, in acetate–phosphate–borate buffers 30 mM. Similar data for oxy-HbGp are reported in Ref. [11].

temperature was defined at 56 °C at pH 7.0, where the scattering particle dimension changed drastically, suggesting the appearance of aggregates in solution as a result of the denaturation process.

At pH 8.0 and 9.0, a decrease of $<D_h>$ is associated to the temperature-induced protein oligomeric dissociation, followed by an increase of $<D_h>$, which is gradual and starts at a higher temperature, as compared to the temperature for protein dissociation. The temperatures of the beginning of the dissociation and denaturation processes (T_{diss} and T_{den}, respectively) are included in Table 1. It is clear that the dissociation is not complete and that the beginning of the denaturation overlaps with the dissociation. Table 1 also includes the minimal $<D_h>$ values observed in the melting curves (Fig. 2). The variation of T_{diss} as a function of pH is consistent with the data on pH stability, shown in Fig. 1: on going from pH 8.0 to pH 9.0, T_{diss} reduces from 45 °C to 38 °C. The values of $<D_h>$ at the highest temperature (70 °C) are higher at pH 7.0 (minimum of 100 nm), as compared to the more alkaline pH 8.0–9.0 (29–18 nm). The lowest value of $<D_h>$ at pH 8.0 is also higher than the observed for oxy-HbGp, which is around 12 nm and corresponds to a more extensive oligomeric dissociation. The fact that lowering the temperature back to 25 °C, after heating to 70 °C, does not lead to a change in the final value of $<D_h>$ further indicates that the temperature-induced protein dissociation is an irreversible process.

The higher critical denaturation and dissociation temperatures indicate that cyanomet-HbGp is more stable than the oxy-form [11]. At pH 7.0, the denaturation temperature for cyanomet-HbGp is also higher as compared to oxy-HbGp. In the alkaline pH range, cyanomet-HbGp shows also dissociation temperatures higher as compared to those for oxy-HbGp. This observation is in agreement with previous work on oxidized HbGp [16,17].

3.2. Thermal stability by optical absorption spectroscopy studies

In order to obtain some additional information on the denaturation/aggregation process, a simple experiment was performed using optical absorption spectroscopy. Samples of HbGp, in the two oxidation forms, oxy- and cyanomet-HbGp, at 0.5 mg/ml, were heated at 50, 60 and 70 °C, for 1 h. The absorption spectra were obtained at 25 °C, prior to the heating, and after heating and subsequent re-equilibration back at 25 °C. Samples were monitored at pH values 8.0, 9.0 and 10.0. In Fig. S1 of the Supporting Material the results for oxy- and cyanomet-HbGp are presented for the experiments at pH values 8.0 and 9.0. Simple visual inspection of the samples showed the absence of protein aggregation for all pH values in the whole temperature range from 50 to 70 °C. Nevertheless, all samples were centrifuged after the heating/re-equilibration cycle, at 3000 × *g*, prior to the spectral measurements. The analysis of the absorption spectra of oxy-HbGp (see Fig. S1A and S1C) show that the Soret band maximum wavelength shifted from 415 nm to 410–411 nm at pH values 8.0 (Fig. S1A) and 9.0 (Fig. S1C). The corresponding absorbance values, both for the Soret and Q-bands (Fig. S1B, S1D), are reduced to 60% of their original values at 25 °C, after the treatment at 70 °C (data not shown). The percentages obtained for the oxy-HbGp, remaining in solution after heating at 60 and 70 °C, and for the pH range 8.0–10.0, suggest that aggregation and precipitation are not as significant, at alkaline pH values, as for acidic pH or for pH 7.0, as observed recently [17]. For cyanomet-HbGp (see Fig. S1E and S1G) the Soret band maximum, which is around 420 nm at 25 °C, also displays wavelength shifts quite similar to those observed for oxy-HbGp. Heating to 70 °C reduces the absorbances to 52% of the value at 25 °C, at pH values 8.0–10.0. Here, again, the thermal stability at alkaline pH values is comparable for the two oxidation forms. Overall, and in agreement with data from DLS melting studies, HbGp is very stable at 25 °C, undergoing denaturation in the temperature range between 50 and 60 °C. The aggregation/precipitation above 60 °C, which is evident at acidic pH values [17], for both oxidation forms, does not appear to be significant at alkaline pH.

Table 1
Values of the sizes and critical temperatures associated to the effects of temperature and protein concentration on oxy- and cyanomet-HbGp Z-average hydrodynamic diameter ($<D_h>$) at different pH values. The melting points were obtained from the data on Figs. 2 and 3.

[HbGp] mg/ml	T_{diss}(°C)	$<D_h>_{diss}$ (nm)	$<D_h>_{min}$ (nm)	T_{den}(°C)	$<D_h>_{den}$ (nm)
Oxy-HbGp					
pH 7.0					
0.25	–	–	–	52 ± 1	57 ± 3
0.50				52 ± 1	80 ± 6
0.75				52 ± 1	70 ± 4
1.0	–	–	–	50 ± 1	189 ± 6
2.0	–	–	–	50 ± 1	398 ± 20
pH 8.0					
0.25	42 ± 1	26 ± 1	10 ± 1	47 ± 1	16 ± 2
0.50	41 ± 1	27 ± 1	12 ± 1	47 ± 1	26 ± 1
0.75	44 ± 1	26 ± 1	13 ± 1	48 ± 1	28 ± 2
1.0	47 ± 1	26 ± 1	16 ± 1	50 ± 1	35 ± 2
2.0	46 ± 1	26 ± 1	16 ± 1	51 ± 1	39 ± 5
pH 9.0					
0.50	31 ± 1	24 ± 1	11 ± 1	37 ± 1	130 ± 10
Cyanomet-HbGp					
pH 7.0					
0.50	–	–		56 ± 1	100 ± 5
pH 8.0					
0.50	45 ± 1	27 ± 1	17 ± 1	52 ± 1	29 ± 2
pH 9.0					
0.50	38 ± 1	25 ± 1	12 ± 1	45 ± 1	18 ± 2

T_{diss} critical dissociation temperature (beginning of the dissociation process); T_{den} critical denaturation temperature (beginning of the denaturation process); $<D_h>_{diss}$ Z-average hydrodynamic diameter at the beginning of the dissociation; $<D_h>_{den}$ Z-average hydrodynamic diameter at the highest temperature (70 °C), $<D_h>_{min}$ Z-average hydrodynamic diameter at the minimum of the melting curves.

3.3. Protein concentration effect upon thermal stability of HbGp by DLS

Additional information on HbGp thermal stability was obtained from the protein concentration dependence of the melting curves as monitored by DLS. In Fig. 3A and B, data are shown for experiments performed for oxy-HbGp samples at pH 7.0 and 8.0, respectively, in the protein concentration range from 0.25 to 2.0 mg/ml, upon heating from 25 to 70 °C. The high thermal stability of oxy-HbGp at pH 7.0 is again evident (Fig. 3A), as no oligomeric dissociation is observed in the concentration range used. However, an apparent shift of the denaturation temperature, T_{den}, to lower temperatures is observed as the protein concentration is increased. At the same time, the size of the aggregates observed at high temperatures increases (Table 1). These observations can be explained as due to the increase in the tendency of the protein to form aggregates upon denaturation, which causes this apparent shift of the melting curve to lower values of T_{den}. In Fig. 3B, data are shown for the effect of protein concentration at pH 8.0. It is also clear that, at this pH, the protein becomes more stable at higher concentrations, as monitored by the increase in T_{diss} with the increase in protein concentration (Fig. 3B, Table 1). Regarding protein aggregation beyond the denaturation, the trend at pH 8.0 is similar to that at pH 7.0: the higher the protein concentration the higher the size of the aggregates. The corresponding values of critical parameters are also shown in Table 1. Similar experiments were additionally made for cyanomet-HbGp (data not shown). At pH 7.0, and differently from oxy-HbGp, for the cyanomet-form the increase in protein concentration is not accompanied by any change in the value of T_{den}. It remains the same as obtained for 0.5 mg/ml (see Table 1). However, the size of the aggregates formed upon denaturation also increased with the increase of protein concentration. At pH 8.0, oligomeric dissociation is observed in the whole protein concentration range: the smaller the protein concentration the lower the value of T_{diss}.

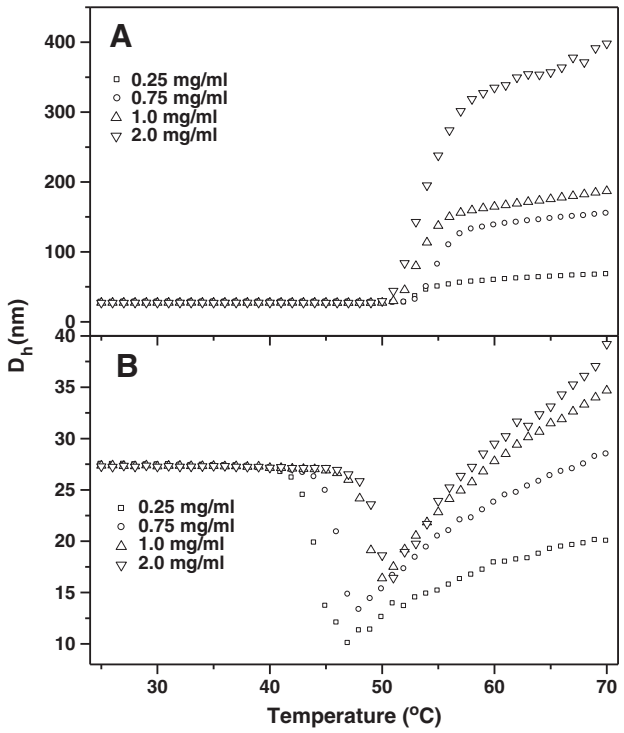

Fig. 3. Effect of the temperature and of the HbGp concentration on the oxy-HbGp hydrodynamic radius, in acetate–phosphate–borate buffers, 30 mM at pH 7.0 (A) and pH 8.0 (B).

Detailed studies regarding the mechanisms of protein aggregation beyond its denaturation are outside the scope of the present study and will be an interesting matter for future studies.

3.4. Kinetics of dissociation by DLS

The thermal stability of cyanomet-HbGp is also significantly higher as compared with the oxy-form. Attempts to follow the dissociation kinetics were not successful. In the temperature range from 44 to 48 °C, at pH 8.0, the protein presented only a slight decrease of $<D_h>$ from 27–28 nm to 24 nm in the initial 2 h, followed by $<D_h>$ oscillations and gradual increase for longer times, up to 24 h. It is worth of notice that at pH 8.0 the value of $<D_h>_{min}$ obtained from an experiment of melting, is 17 nm (Table 1), implying that the dissociation of cyanomet-HbGp, as monitored by DLS, was not complete. For this reason, kinetic studies in this work were performed only for the oxy-HbGp at different temperatures.

Dissociation rate constants progressively increase at higher pH and temperature. The Z-average diameter observed for oxy-HbGp at pH values 7.5 and 8.0, in the temperature range from 38 to 48 °C, followed during the initial 1 h, was 27 ± 1 nm, which is in agreement with the previous work reported for oxy-HbGp, at 25 °C [11]. Measurements for these samples were performed for longer times, up to 20 h, at the lower temperature of 38 °C. Table 2 summarizes the DLS results obtained for the oxy-HbGp, at pH 7.5 and 8.0, at different temperatures. The end of the kinetics curves is, generally, associated with a plateau region, where no significant variation of particle diameter with time is observed. At pH 8.0 and 38 °C, the hydrodynamic diameter observed at the end of the kinetics is 18.6 nm (corresponds to the last 1.5 h, Table 2). At pH 8.0 and 40 °C, D_h is 17.2 nm (last 1.5 h, Table 2). In the temperature range from 38 to 40 °C, at pH 8.0, the kinetics was monitored for 22.5 h and no sign of protein aggregation was observed. However, the aggregation phenomenon was noticed with the increase of the temperature: at pH 8.0 the aggregation was evident above 41 °C, while at pH 7.5 this phenomenon was clear above 43 °C. Lowering the pH leads to a slight increase in the temperature necessary to promote protein aggregation. This aggregation effect was not observed for the dissociation kinetics monitored at alkaline pH for the oxy-HbGp at 25 °C [11]. Therefore, higher temperatures promote oligomeric dissociation, followed by protein denaturation and aggregation that might mask the oligomeric dissociation, as the partial dissociation will be overlapped with the start of the denaturation and subsequent aggregation. This can be seen from the fact that at the end of the kinetic curves, monitored in this work, the particle diameters observed (see Table 2), in average, are higher than those observed at alkaline pH (~ 10 nm) [11].

Fig. 4A shows the variation of the hydrodynamic diameter as a function of time for oxy-HbGp at pH 8.0 and 43 °C. It is noticed that the oligomeric structure is not completely dissociated ($D_h = 14.2$ nm). After 6–7 h, at least three phenomena start to occur simultaneously: temperature-induced oligomeric dissociation, protein denaturation and protein aggregation. Fig. 4B and C show the dependences of the hydrodynamic diameters of the protein on time, assessing its oligomeric dissociation, denaturation and aggregation based on the scattering intensity (Fig. 4B) and on the number of scattering particles (Fig. 4C). In these figures, a clear indication of the dissociation process can be observed. An initial decrease of the diameter, from 27 to 18 nm is observed after 4 h (Fig. 4B and C). The time interval from 6 to 8 h yields a constant D_h value of 14 nm. In Fig. 4B the contribution of large particles (D_h ~240 nm) is observed, indicating the start of a protein aggregation phenomenon accompanying the protein denaturation. The width of the particle size distribution for dissociated oxy-HbGp may be characterized by the polydispersion index (PDI, Table 2). After 18 h, the particle size is 20 nm, with a higher PDI. The analysis of DLS data using relative scattering intensity (Fig. 4B) and relative scattering particle number (Fig. 4C) yield similar results.

The kinetic studies reported above on the thermal dissociation of the oxy-HbGp at pH 7.5 and 8.0, as a function of temperature, were carried out at the temperatures and time range preceding the denaturation and accompanying aggregation phenomena. The dissociation model, described previously for the measurements at 25 °C [11] was used in this work. Fig. 5 shows the experimental results, at pH 8.0, together with the fittings of the kinetic curves to Eq. (2), as a mono-exponential process. The rate constants and diffusion coefficients are collected together in Table 2 for pH 7.5 and 8.0. The dissociation is slow at pH 8.0 and 38 °C ($k = 0.72 \times 10^{-4}\ s^{-1}$, Table 2), taking approximately 23 h for the process to be completed. The dissociation rate progressively increases at higher temperature ($k = 8.2 \times 10^{-4}\ s^{-1}$ at 45 °C, Table 2), being eleven-fold higher on going from 38 °C to 45 °C, at pH 8.0. At pH 7.5 and 42 °C, the rate constant (Table 2) value obtained from the fittings of the kinetic curves (data not show) is $k = 1.84 \times 10^{-4}\ s^{-1}$, which is a factor of 1.6 lower than that obtained at pH 8.0 for the same temperature. In this way, the dissociation rate increases for higher pH and temperature values, being the effect of temperature more pronounced. The highest value of rate constant obtained for oxy-HbGp at 25 °C, at pH 10.1 [11], is, approximately, the double of the highest value observed in the present work for the highest temperature (45 °C).

It is important to notice that our DLS data did not allow the determination of the rate constants associated to the intermediate step(s) of the protein dissociation [11]. Thus, the value of the rate constant obtained in this study is related to the conjugation of all phases, or to the limiting step of the simple oligomeric dissociation model previously proposed [11].

In order to determine the activation energy (E_a) for the oxy-HbGp oligomeric dissociation, the rate constants values as a function of temperature for oxy-HbGp were analyzed. The Ahrrenius plots of the dissociation rates as a function of inverse temperature are shown in Fig. 6. E_a values obtained from Arrhenius plots by DLS were 262 and 278 kJ/mol, at pH 8.0 and 7.5, respectively. The results confirmed that

Table 2
Dissociation kinetic constants for oxy-HbGp at different temperatures and pH values.

Parameters	Data obtained for each temperature and pH							
pH 8.0								
T (°C)	38	39	40	41	42	43	44	45
D_h(nm)*	18.6	16.6	17.2	15.8	14.3	14.2	14.7	13.5
PDI	0.43	0.36	0.32	0.25	0.31	0.33	0.43	0.35
$D_p(\times 10^{-12}\ m^2s^{-1})$	2.42	2.4	2.59	2.65	2.70	2.80	2.85	2.79
D_∞ $(\times 10^{-12} m^2s^{-1})$	4.04 ± 0.03	3.95 ± 0.02	4.45 ± 0.01	4.81 ± 0.01	5.33 ± 0.02	5.34 ± 0.02	5.64 ± 0.02	6.22 ± 0.06
k $(\times 10^{-4}\ s^{-1})$	0.72 ± 0.02	1.36 ± 0.03	1.58 ± 0.03	1.91 ± 0.03	3.0 ± 0.1	4.0 ± 0.1	5.8 ± 0.4	8.2 ± 0.4
R^2	0.99	0.98	0.98	0.99	0.99	0.99	0.96	0.99
N	459	490	456	370	184	169	73	45
pH 7.5								
T (°C)	42	43	44	45	46	47	48	
D_h(nm)*	19.5	18.9	18.4	18.6	17.1	16.7	15.6	
PDI	0.24	0.23	0.22	0.25	0.21	0.21	0.24	
$D_p(\times 10^{-12}\ m^2s^{-1})$	2.69	2.76	2.8	2.84	2.93	2.99	3.02	
D_∞ $(\times 10^{-12} m^2s^{-1})$	3.46 ± 0.01	4.06 ± 0.02	4.27 ± 0.02	4.62 ± 0.04	4.37 ± 0.03	5.13 ± 0.06	5.29 ± 0.01	
k $(\times 10^{-4}\ s^{-1})$	1.84 ± 0.05	2.0 ± 0.1	2.4 ± 0.2	3.4 ± 0.2	6.0 ± 0.4	7.1 ± 0.4	9 ± 1	
R^2	0.99	0.97	0.98	0.98	0.97	0.98	0.91	
N	462	351	233	141	110	63	48	

* These values of diameter correspond to the particle dimensions at the end of the kinetics. N corresponds to the number of experimental points. The second and third lines, for each pH value, correspond to the parameters obtained at the end of the kinetics. The fourth line corresponds to the initial diffusion coefficients obtained from DLS experimental data.

a slightly higher energy is necessary to dissociate the oligomer at lower pH, as a result of the higher stability of the protein at less alkaline pH values.

As mentioned above, detailed studies regarding the mechanisms of protein aggregation beyond its denaturation are outside the scope of the present study and will be an interesting matter for future studies. However, since the increase in the protein concentration leads to an increase in the critical oligomeric dissociation temperature, an increase in activation energy is expected for higher HbGp concentration.

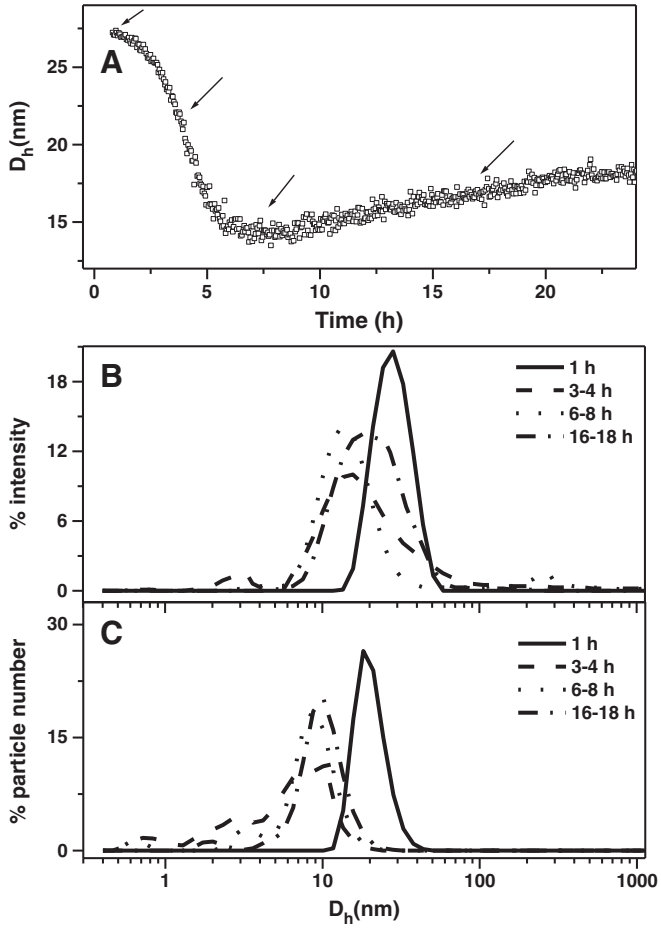

Fig. 4. (A) Kinetics of dissociation of oxy-HbGp 0.5 mg/mL, at pH 8.0, in acetate–phosphate–borate buffer 30 mM, at 43 °C. The arrows indicate the moments in the kinetics where the distributions of scattering particle were chosen. (B) Intensity particles size distributions and (C) number of particles size distribution at the different moments of the kinetics indicated in (A).

3.5. Auto-oxidation kinetics by optical absorption

Auto-oxidation kinetic decays of oxy-HbGp were monitored through the absorbance at 415 nm as a function of time in acetate–phosphate–borate 30 mM, pH 8.0, in the temperature range from 38 to 44 °C. The auto-oxidation kinetics monitored by UV–VIS presents a mono-exponential behavior [11,19].

In Fig. S2A, in the Supporting Material, examples of kinetic data obtained at different temperatures are shown. The rate constants, k_{obs}, for oxy-HbGp at pH 8.0, for the temperatures 38, 40, 42, 43 and 44 °C were 1.5×10^{-5}, 2.5×10^{-5}, 5.7×10^{-5}, 1.3×10^{-4} and 1.6×10^{-4} s^{-1}, respectively. The rate constant at pH 8.0 and 38 °C is a factor of 33 lower than that at pH 9.0 at the same temperature [11,19]. This is an indication that the auto-oxidation at alkaline pH is faster. On the other hand, the values of k observed in DLS experiments are a factor of 5.0 higher as compared to those from auto-oxidation at pH 8.0 and 38 °C. Auto-

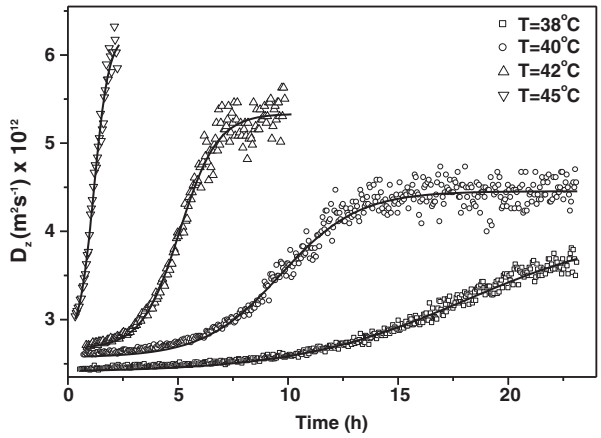

Fig. 5. Dissociation kinetic decays (symbols) and fits (full lines) of oxy-HbGp at indicated temperatures. DLS data were monitored as a function of time in acetate–phosphate–borate 30 mM buffer pH 8.0, at different temperatures. [HbGp] = 0.5 mg/ml. DLS kinetic Z-average diffusion coefficients were fitted to Eq. (2) to obtain the characteristic rate constant values k. All parameters from the fits are presented in Table 2.

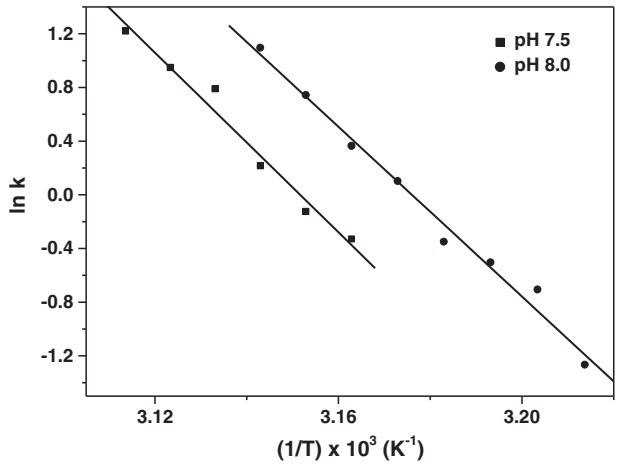

Fig. 6. Arrhenius plots for the dissociation of oxy-HbGp. The dissociation rates of oxy-HbGp were measured at 0.5 mg/mL, in acetate–phosphate–borate 30 mM, at pH 7.5 and 8.0, by DLS. The lines are the linear best fits at indicated pH values.

oxidation kinetic experiments monitor the accessibility of the heme groups upon their exposure to the solvent. Thus, this process is linked to the maintenance of the overall oligomeric protein structure, while, on the other hand, DLS kinetic experiments are sensitive, primarily, to the average sizes of the scattering particles in solution [11]. The process that prevails initially is the oligomeric dissociation, consequently originating a more pronounced auto-oxidation due to the increased accessibility of the heme pockets on the dissociated protein. This explains the higher rate constant obtained by DLS data as compared to the values from UV–VIS.

The rate constant values obtained at different temperatures are presented as Arrhenius plots in Fig. S2B. The activation energies for the auto-oxidation reactions were estimated, being equal to 333 kJ/mol (see Table S1 in Supporting Material). Previous work has evaluated the activation energies for the auto-oxidation of HbGp in the integral form and as the pure monomer subunit *d*, both at pH 9.0 [19]. These reported values are roughly half of the obtained in the present work (Table S1), suggesting that the oligomeric dissociation of HbGp, as well as the related auto-oxidation reactions, are less efficient at pH 8.0 as compared to pH 9.0. It is also worth of notice, that at pH 9.0, a bi-exponential behavior takes place at 38 °C [11,19], while at pH 8.0 (this work) a mono-exponential decay is observed, consistent with the indistinguishable oxidation (and accessibility of the heme to the solvent) of all hemoglobin subunits at this lower pH.

3.6. Differential scanning calorimetry (DSC)

3.6.1. Effect of heating scan rate

Fig. 7 shows the DSC heating scans for oxy-HbGp (Fig. 7A) and cyanomet-HbGp (Fig. 7B), at pH 7.0, and for several scan rates in the range from 0.5 to 1.5 °C/min. The first heating scan is shown because the denaturation is irreversible for HbGp, in both oxidation forms. The re-heating scans contained no transition peaks, and the post-transitional baselines at the end of the first heating scans showed no signs of sample aggregation at the investigated pH values of 7.0 and 8.0. The thermal unfolding shown in Fig. 7 is not a simple single two-state transition, as it was not possible to fit the corresponding endotherms using this simple model. To fit the complete experimental endotherm adequately two components were necessary although, for oxy-HbGp at pH 7.0 one component gave a good fit (see Material and methods section). In Fig. 7, it is evident that the position of the mid-point temperatures corresponding to the denaturation process is strongly dependent upon the heating scan rate. The faster the heating scan through the transition, the higher its critical temperature. This observation is consistent with several literature reports [21–26] and

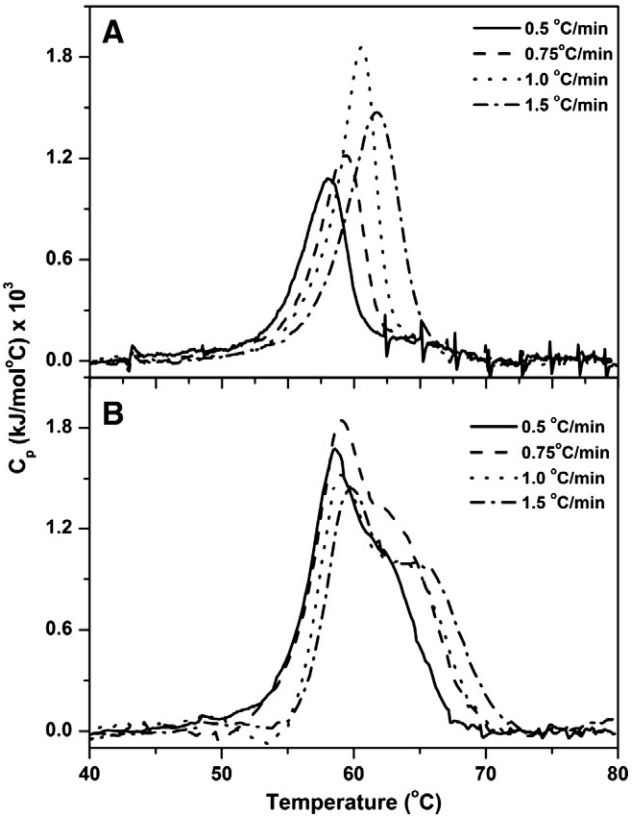

Fig. 7. Experimental DSC thermograms for oxy-HbGp (A) and cyanomet-HbGp (B) at pH 7.0, and at different indicated scan rates in the range from 0.5 to 1.5 °C/min. [HbGp] = 0.5 mg/mL.

suggests that the denaturation process in HbGp is kinetically controlled. It is also worth of notice that all endotherms for oxy-HbGp, at pH 7.0 (Fig. 7A), start to give an appreciable value of C_p at temperatures in the range 50–55 °C. This beginning of the endotherm coincides with the denaturation temperature observed in DLS melting studies, described above. Moreover, the endotherms for cyanomet-HbGp, at pH 7.0 (Fig. 7B), look broader and more asymmetric, as compared to those for oxy-HbGp (Fig. 7A). This suggests that for cyanomet-HbGp there are at least two quite different domains undergoing denaturation at different temperatures. One of these domains has a higher denaturation temperature as compared to oxy-HbGp (Fig. 7B, see also Table 3). The alternative possibility is that for oxy-HbGp, at pH 7.0, the oligomeric dissociation is so fast that it does not have a limiting effect upon the protein denaturation, while for cyanomet-HbGp the oligomeric dissociation is not as fast and manifests itself in the more complex endotherm.

3.6.2. Effect of protein concentration

Denaturation of oligomeric proteins can include an intermediate step associated to a reversible dissociation into smaller subunits (monomers, dimers, trimers, etc.). In such a case, the $C_p \times T$ profile can become dependent on protein concentration. The role of dissociation and association reactions in the mechanism of thermal denaturation of oxy-HbGp was tested by monitoring DSC curves at various proteins concentrations. As can be seen in Fig. 8, varying the protein concentration in the range from 0.5 to 2.0 mg/ml affects the shape and height of the main peak.

At pH 7.0 (Fig. 8A), a shift of T_m to higher temperatures is observed as the protein concentration is increased. A well defined relatively narrow peak is observed for this condition. The initial denaturation temperature in the endotherm for 0.5 mg/ml is 55 °C, and the temperature corresponding to the center of the peak (C_p maximum),

Table 3
Activation energies and melting temperatures for oxy- and cyanomet-HbGp at pH 7.0 and 8.0 obtained from DSC data, at a scan rate of 1 °C/min and 0.5 mg/ml of protein.

pH values	T_{m1}(°C)	E_{a1} (kJ/mol)	T_{m2} (°C)	E_{a2} (kJ/mol)	T_{m3}(°C)	E_{a3} (kJ/mol)	$E_{a\ (Total)}$ (kJ/mol)
oxy-HbGp							
7.0	60.2 ± 0.5	260 ± 15			–	–	260 ± 15
8.0	50.6 ± 0.3	339 ± 34	58.9 ± 0.1	196 ± 36			535 ± 70
cyanomet-HbGp							
pH 7.0	60.1 ± 0.2	453 ± 90	65.3 ± 0.2	386 ± 31		–	839 ± 121
pH 8.0	52.1 ± 0.2	561 ± 171	60.7 ± 0.3	288 ± 32		–	849 ± 203
Rapana thomasiana hemocyanin[a]							
pH 7.2	83	597 ± 20	90	615 ± 25			1212 ± 45
Concholepas concholepas hemocyanin[b]							
pH 7.2	81.6 ± 0.1	323 ± 2	84.4 ± 0.2	563 ± 5	94.3 ± 0.3	322 ± 5	1208 ± 12

[a] Data from Ref. [12].
[b] Data from Ref. [28].

T_m, is 60 °C; for 2.0 mg/ml the initial denaturation temperature is shifted to 57 °C, and T_m is also shifted to 66 °C. At pH 8.0 (Fig. 8B), the shape of the endotherms is different as compared to that observed at pH 7.0: the endotherms become very wide, the main peak is shifted to lower temperatures, and T_m is shifted to higher temperatures as the protein concentration is increased. Besides that, a clear effect of reduction of the temperature range (narrowing) is seen for the endotherms, especially for that at 2.0 mg/ml. The effects of the protein concentration described above can be explained assuming that at low concentrations (0.5 mg/ml, Fig. 8B) a significant oligomeric dissociation takes place for oxy-HbGp at pH 8.0, leading to significant denaturation of the smaller subunits at lower temperatures, starting from 40–42 °C. At 2.0 mg/ml (Fig. 8B), this dissociation is more limited and most of the heat effect takes place simultaneously for the partially dissociated oligomer: the heat effect starts, in this case, around 50 °C. This result is very consistent with DLS data reported in Fig. 3B. In this way, oligomeric dissociation at alkaline pH 8.0 manifests itself in DSC scans as a significant lowering of T_m, simultaneously with a broadening of the endotherms. The existence of protein concentration dependence for the irreversible transition indicates that oligomeric dissociation is part of the rate-determining irreversible reaction. Thus, the lower temperature component in the endotherm could be associated to the oligomeric dissociation.

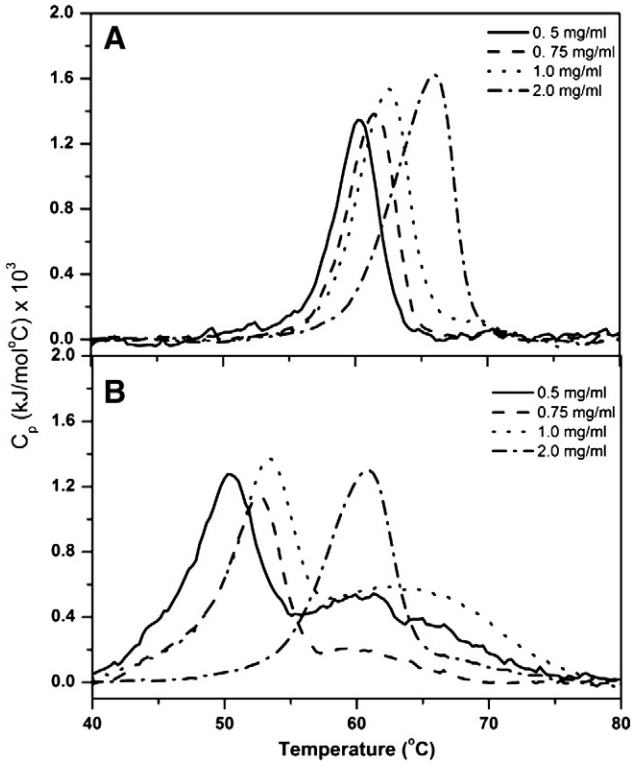

Fig. 8. Experimental DSC thermograms for oxy-HbGp at pH 7.0 (A) and pH 8.0 (B), and at different concentration of HbGp in the range from 0.5 to 2.0 mg/ml. The scan rate was 1.0 °C/min.

3.6.3. Estimation of activation energy (E_a)

DSC experiments at a fixed protein concentration of 0.5 mg/ml, and at several scan rates in the range from 0.5 to 1.5 °C/min, for oxy- and cyanomet-HbGp, at pH 7.0 and 8.0, were performed aiming to estimate the activation energy for the denaturation of HbGp. Based on these data, it is possible to estimate an activation energy for the denaturation/unfolding, as discussed in several reports in the literature by Sanchez-Ruiz et al. [21,22,25,26]. In Fig. 9 plots are presented for the dependence of $\ln\left({}^{v}/_{T_m^2}\right)$ versus ${}^{1}/_{Tm}$ according to the equation:

$$\ln\left(v \Big/ T_m^2\right) = c - E_a \Big/ RT_m \tag{4}$$

where v is the heating scan rate, T_m is the mid-point transition temperature, E_a is the activation energy for the rate-limiting process of denaturation, c is a constant and R is the gas constant. The number of plots in Fig. 9 corresponds to the number of components necessary to fit the whole endotherms (see Material and methods section) shown in Fig. 7. The mid-point temperatures of the component peaks are listed in Table 3, together with the activation energies estimated from the data regarding the different scan rates (Eq. (4) and Fig. 9) and described above.

In general, thermodynamic parameters can be obtained and are well defined for reversible denaturation transitions [22]. According to the Lumry and Eyring model [22,25–27], the irreversible denaturation of proteins is suggested to involve at least two steps. The first step is a reversible unfolding of the native protein N. This is followed by an irreversible change of the denatured protein into a final irreversible state, F, which cannot fold back into the native state:

$$N \underset{k_{-1}}{\overset{k_1}{\rightleftharpoons}} D \overset{k_2}{\rightarrow} F \tag{5}$$

A special case of the Lumry and Eyring model is when $k_2 >> k_{-1}$, where most of the D molecules will be converted to F, as an alternative to refolding back to the native state. In this case, the denaturation process can be regarded as a one-step process following first-order kinetics:

$$N \overset{k}{\rightarrow} F \tag{6}$$

This model forms the basis of the elaborate treatments of irreversible DSC measurements by Sanchez-Ruiz and collaborators [21,22,25,26]. Furthermore, it has been used for the interpretation of DSC data from the thermal denaturation of several hemocyanins [12,28].

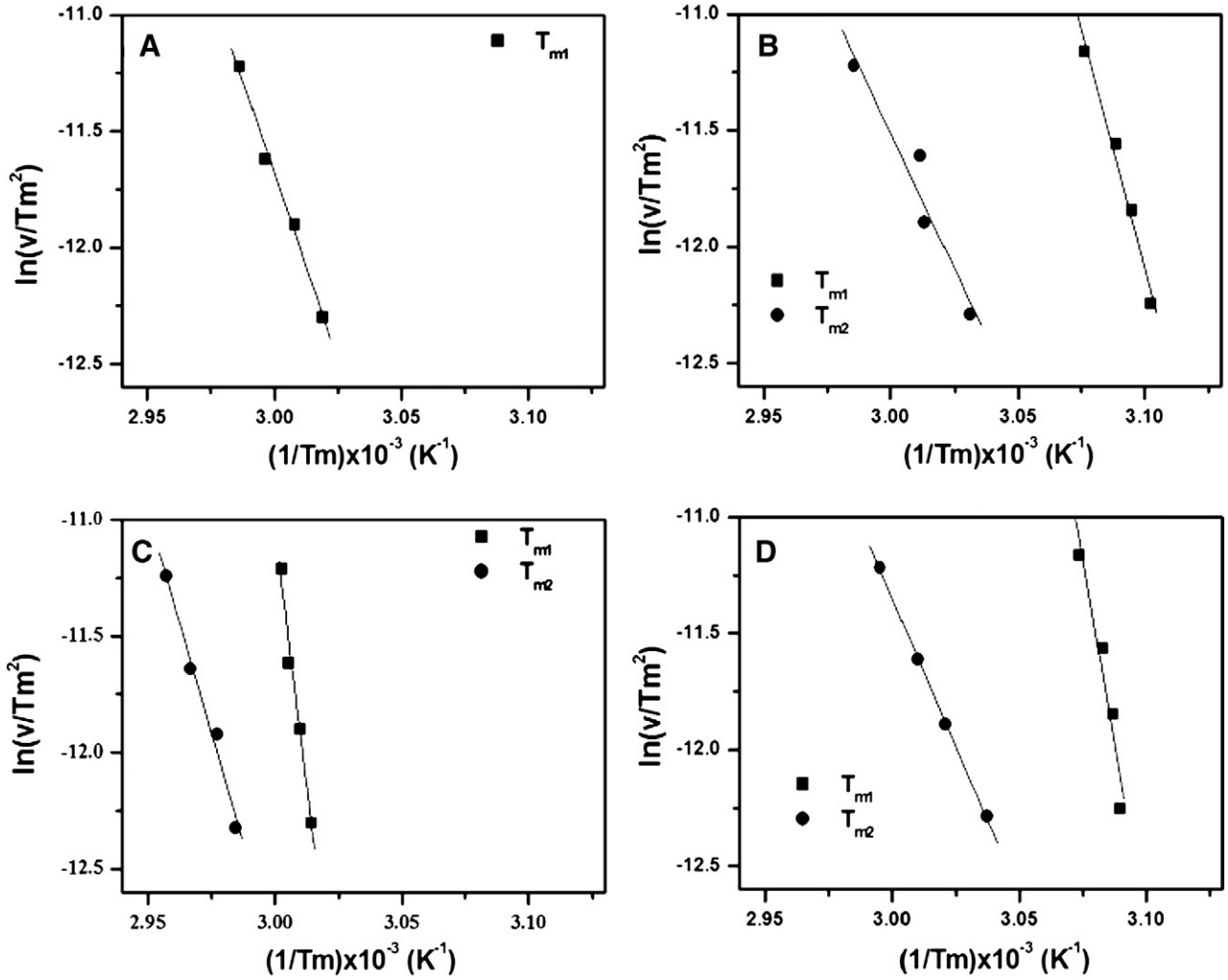

Fig. 9. Arrhenius plots for the irreversible thermal denaturation of oxy-HbGp at pH 7.0 (A) and 8.0 (B), and of cyanomet-HbGp at pH 7.0 (C) and 8.0 (D). [HbGp] = 0.5 mg/mL. The different symbols correspond to the mid-point transition temperatures T_{m1} and T_{m2}, obtained by fitting the whole endotherm into components associated to independent transitions. The lines are the best linear fits of the Arrhenius plots. The values of the activation energies are presented in Table 3.

In the present case, for the irreversible denaturation of the oligomeric HbGp described above, the two-state irreversible model of Sanches-Ruiz et al. [21,22,25–27] could provide an approximate representation of our DSC data, even if the real mechanism of thermal denaturation is expected to have a more complex character than the simple one-step transformation.

The dependence of the denaturation on the protein concentration, described above, suggests that the oligomeric dissociation is part of the rate-limiting step, exerting a kinetic control of the denaturation process. This is reflected in the differences between the thermal stabilities of the oxy- and cyanomet-HbGp, observed from DSC data (one component versus two components, respectively, at pH 7.0), which are consistent with data from DLS (higher protein concentrations leads to higher critical dissociation temperature). The quantitative evaluation of the denaturation process for HbGp allows the comparison of our results with those obtained by DSC measurements of hemocyanins [12,28] as well as with other proteins. In this context, it is also worth of notice the work on denaturation and aggregation of ovalbumin described by Weijers et al. [29]. The denaturation process at neutral pH 7.0 is described by irreversible first-order kinetics, being independent of protein and salt concentrations, but strongly temperature dependent. The authors propose that protein aggregation takes place after the transition from the native to the denatured states. Since no protein concentration dependence is observed, in this case oligomerization is not affecting the denaturation process. Arrhenius plots were obtained with activation energies in the range 430–490 kJ/mol.

Also of interest in the present context is the work conducted by Fodor et al. [20] with Na,K-ATPase, where the irreversible denaturation was monitored under several experimental conditions. A broad endotherm was obtained, which did not correspond to a single two-state transition and could only be completely fitted by up to four components. The heats of transition, ΔH_d, and mid-point temperatures, T_d, were estimated for these components and their changes evaluated as a function of the mechanical stress upon the enzyme and presence of salts in solution. Besides the comparison of our DSC data with literature reports, the present analysis allows a comparison of the additional data obtained by different techniques in the present work, especially our DLS results. Additional quantitative data reported in the literature for two hemocyanins from different species were also included in Table 3. Of course, caution is necessary for these comparisons since the mechanisms and the precise origin of these changes are not known and, for this reason, they could be different for different proteins.

However, the comparison with our data for HbGp is quite interesting: first of all, in the case of the hemocyanins, the presence of more than one structural domain undergoing thermal unfolding more or less independently of each other was used as an explanation

for the observed data [28]. However, our data for HbGp could be also rationalized as due to the presence of oligomeric dissociation as a step in the kinetically controlled denaturation process. Moreover, the transition temperatures for the hemocyanins reported in the literature, and added to Table 3, are at least 20 °C higher as compared to HbGp. This suggests that the hemocyanins have a thermal stability higher than that of HbGp. The activation energy values in Table 3 are also consistent with this behavior, since HbGp presents values systematically lower than those for hemocyanins. The presence of two components in the HbGp endotherms suggests that the oligomeric dissociation occurs at a slightly lower temperature than the protein denaturation. This becomes especially evident in Fig. 8, where the endotherms of oxy-HbGp at pH 8.0 become broader and the values of T_m shift to lower temperatures. In Table 3 data are shown for the activation energies and transition temperatures for both oxy- and cyanomet-HbGp at pH 7 and 8. It is noticed that for oxy-HbGp, at pH 7, a single activation energy of 260 kJ/mol is observed with a mid-point transition temperature of 60.2 °C. On going to pH 8, two values of activation energy and transition temperatures are observed with a total activation energy value of 535 kJ/mol. Based on our observations from DLS data, the first value could be associated to the oligomeric dissociation, while the second one corresponds to the protein denaturation. It is interesting that for cyanomet-HbGp, two activation energy values are obtained for both pH values, with a total E_a value of 840 kJ/mol, significantly higher as compared to oxy-HbGp. This observation reflects, probably, the higher stability of HbGp both towards oligomeric dissociation as well as protein denaturation for the cyanomet-form. It will be quite interesting for future studies to monitor the thermal behavior of isolated HbGp subunits to compare their stability with that of the whole protein investigated in the present report.

4. Conclusions

The characterization of the stability of HbGp and of the pH- and temperature-induced destabilization of its quaternary structure, as well as the reciprocal effects of temperature on pH stability and pH on temperature stability, are of key importance for the development of mimetic systems of this protein and other erythrocruorins to be used as artificial blood substitutes [11]. Additionally, the changes on these parameters, their kinetics and thermodynamics upon heme reduction also need to be taken into account.

Cyanomet-HbGp is more stable as compared to oxy-HbGp, based on its higher critical denaturation and dissociation temperatures, as observed from the melting curves. Besides that, the cyanomet-form is thermally very stable, since in the temperature range from 44 to 48 °C, at pH 8.0, only a slight partial dissociation is observed, leading to a scattering particle size change from 27–28 nm to 24 nm. This observation of a higher thermal stability, together with the fact that an aggregation phenomenon takes place upon heating of the protein up to temperatures near the critical denaturation temperature, precluded the determination of the activation energy for this species. It is interesting that the dissociation of cyanomet-HbGp was observed in the DLS melting experiments going beyond the denaturation temperature, while at a fixed temperature below the critical dissociation/denaturation the dissociation process was not observed by DLS. This again could be explained by the very critical dependence of HbGp denaturation on a rate-limiting kinetically controlled process, which is more sensitive for the cyanomet-form. This higher sensitivity for this oxidation form also manifests itself in DSC experiments, where endotherms are observed at pH 7.0 with two components.

Auto-oxidation and dissociation processes are related, so that oligomeric protein dissociation promotes the increase of auto-oxidation rate and vice-versa. Activation energies for oxy-HbGp dissociation obtained from DLS (262–278 kJ/mol) and for auto-oxidation from optical absorption spectroscopy (333 kJ/mol) are comparable. At pH 8.0, dissociation becomes slightly easier as compared to pH 7.5. Our activation energy estimates suggest also that oligomeric dissociation probably triggers the heme iron oxidation.

The present work shows that DLS can be used to follow, quantitatively, the changes on the oligomerization of multisubunit proteins, including the kinetics and thermodynamics of these processes. It is also shown that oligomeric protein dissociation promotes an increase in auto-oxidation rate and vice-versa.

Finally, results from DSC show that the thermal denaturation of HbGp is an irreversible process, quite similar to that reported for hemocyanins. Besides that, the denaturation is a kinetically controlled process and the activation energy, E_a, corresponding to the rate-limiting step has been evaluated. The values for E_a associated to the individual components observed in the endotherm are comparable to the values observed from DLS and optical absorption. At pH 7.0 a single value of 260 kJ/mol is obtained for oxy-HbGp, while for cyanomet-HbGp two values of 453 and 386 kJ/mol are obtained. Probably, the higher stability of the cyanomet-form makes it oligomeric dissociation slower as compared to oxy-HbGp, and this is manifested in the presence of two components in the endotherm, one associated to the oligomeric dissociation and the second one to the protein denaturation. The higher activation energies for the oxidized form are also consistent with its higher thermal stability. They are also consistent with reported literature values for other globular oligomeric proteins and enzymes.

Acknowledgments

The authors are indebted to Mr Ézer Biazin (Universidade de São Paulo) and Mrs. Teresa Freitas (Universidade de Lisboa) for excellent technical support with sample preparations, and to Dr. Alessandra L. Poli (Universidade de São Paulo) for useful comments regarding UV–VIS kinetic data. The authors are also indebted to Dr. Fernando Mello for help at the initial stage of the work with DSC and to Mrs. Andressa Patricia Alves Pinto for the help with the calorimetric experiments. The authors are grateful to the Brazilian agencies FAPESP, CNPq and CAPES and to the Portuguese FCT-MCTES for partial financial support.

Appendix A. Supplementary data

Supplementary data to this article can be found online at doi:10.1016/j.bpc.2010.08.010.

References

[1] F.A.O. Carvalho, P.S. Santiago, J.C. Borges, M. Tabak, On the molecular mass of the extracellular hemoglobin of Glossoscolex paulistus: analytical ultracentrifugation re-examination, Anal. Biochem. 385 (2009) 257–263.
[2] S.N. Vinogradov, The stoichiometry of the four linker subunits of Lumbricus terrestris hemoglobin suggests an asymmetric distribution, Micron 35 (2004) 127–129.
[3] F. Zal, B.N. Green, P. Martineau, F.H. Lallier, A. Toulmond, S.N. Vinogradov, J.J. Childress, Polypeptide chain composition diversity of hexagonal-bilayer hemoglobins within a single family of annelids, the alvinellidae, Eur. J. Biochem. 267 (2000) 5227–5236.
[4] A. Krebs, P. Zipper, S.N. Vinogradov, Lack of size and shape alteration of oxygenated and deoxygenated Lumbricus terrestris hemoglobin? Biochim. Biophys. Acta 1297 (1996) 115–118.
[5] M.S. Oliveira, L.M. Moreira, M. Tabak, Partial characterization of giant extracellular hemoglobin of Glossoscolex paulistus: a MALDI-TOF-MS study, Int. J. Biol. Macromol. 40 (2007) 429–436.
[6] M. Rousselot, E. Delpy, C.D. La Rochelle, V. Lagente, R. Pirow, J. Rees, A. Hagege, D. Le Guen, S. Hourdez, F. Zal, Arenicola marina extracellular hemoglobin: a new promising blood substitute, Biotechnol. J. 1 (2006) 333–345.
[7] N.C. Meirelles, B. Oliveira, E. de Paula, S. Marangoni, G.M. Rennebeck, Erythrocruorin of Glossoscolex-paulistus (oligochaeta, glossoscolecidae) — dissociation at alkaline pH and its ligand properties as revealed by chemical, immunochemical and electron-microscopy studies, Comp. Biochem. Physiol. 88A (1987) 337–379.
[8] P.D. Martin, A.R. Kuchumov, B.R. Green, R.W.A. Oliver, E.H. Braswell, J.S. Wall, S.N. Vinogradov, Mass spectrometric composition and molecular mass of Lumbricus terrestris hemoglobin: a refined model of its quaternary structure, J. Mol. Biol. 255 (1996) 154–169.

[9] O.H. Kapp, G. Polidori, M.G. Mainwaring, A.V. Crewe, S.N. Vinogradov, The reassociation of Lumbricus-terrestris hemoglobin dissociated at alkaline pH, J. Biol. Chem. 259 (1984) 628–639.
[10] W.E. Royer, H. Sharma, K. Strand, J.E. Knapp, B. Bhyravbhatla, Lumbricus Erythrocruorin at 3.5 angstrom resolution: architecture of a megadalton respiratory complex, Structure 14 (2006) 1167–1177.
[11] P.S. Santiago, F. Moura, L.M. Moreira, M.M. Domingues, N.C. Santos, M. Tabak, Dynamic light scattering and optical absorption spectroscopy study of pH and temperature stabilities of the extracellular hemoglobin of Glossoscolex paulistus, Biophys. J. 94 (2008) 2228–2240.
[12] K. Idakieva, K. Parvanova, S. Todinova, Differential scanning calorimetry of the irreversible denaturation of Rapana thomasiana (marine snail, Gastropod) hemocyanin, Biochim. Biophys. Acta 1748 (2005) 50–56.
[13] K.A. Markossian, I.K. Yudin, B.I. Kurganov, Mechanism of suppression of protein aggregation by α-crystalline, Int. J. Mol. Sci. 10 (2009) 1314–1345.
[14] K.A. Markossian, B.I. Kurganov, D.I. Levitsky, H.A. Khanova, N.A. Chebotareva, A.M. Samoilov, T.B. Eronina, N.V. Fedurkina, L.G. Mitskevich, A.V. Merem'yanin, S.Yu. Kleymenov, V.F. Makeeva, V.I. Muronetz, I.N. Naletova, I.N. Shalova, R.A. Asryants, E.V. Schmalhausen, L. Saso, Yu.V. Panyukov, E.N. Dobrov, I.K. Yudin, A.C. Timofeeva, K.O. Muranov, M.A. Ostrovsky, Protein folding: new research, in: T.R. Obalinsky (Ed.), Mechanism of the Chaperone-Like Activity, Nova Science Publishers, Inc, 2006, p. 89.
[15] S.C.M. Agustinho, M.H. Tinto, J.R. Perussi, M. Tabak, H. Imasato, Fluorescence studies of extracellular hemoglobin of Glossoscolex paulistus in met form obtained from Sephadex gel filtration, Comp. Biochem. Physiol. 118A (1998) 171–181.
[16] S.C.M. Agustinho, M.H. Tinto, H. Imasato, T.T. Tominaga, J.R. Perussi, M. Tabak, Spectroscopic studies of the met form of the extracellular hemoglobin from Glossoscolex paulistus, Biochim. Biophys. Acta 1298 (1996) 148–158.
[17] P.S. Santiago, F.A.O. Carvalho, M.M. Domingues, J.W.P. Carvalho, N.C. Santos, M. Tabak, Isoelectric point determination for Glossoscolex paulistus extracellular hemoglobin: oligomeric stability in acidic pH and relevance to protein-surfactant interactions, Langmuir 26 (2010) 9794–9801.
[18] C.S. Johnson Jr., A. Gabriel, Laser Light Scattering, Dover Publications Inc., New York, 1994.
[19] A.L. Poli, L.M. Moreira, A.A. Hidalgo, H. Imasato, Autoxidation studies of extracellular hemoglobin of Glossoscolex paulistus at pH 9: cyanide and hydroxyl effect, Biophys. Chem. 114 (2005) 253–260.
[20] E. Fodor, N.U. Fedosova, C. Ferencz, D. Marsh, T. Pali, M. Esmann, Stabilization of Na,K-ATPase by ionic interactions, Biochim. Biophys. Acta 1778 (2008) 835–843.
[21] M. Costas, D. Rodriguez-Larrea, L. De Maria, T.V. Borchert, A. Gomez-Puyou, J.M. Sanchez-Ruiz, Between-species variation in the kinetic stability of TIM proteins linked to solvation-barrier free energies, J. Mol. Biol. 385 (2009) 924–937.
[22] J.M. Sanchez-Ruiz, Theoretical analysis of Lumry–Eyring models in differential scanning calorimetry, Biophys. J. 61 (1992) 921–935.
[23] B.I. Kurganov, A.E. Lyubarev, J.M. Sanchez-Ruiz, V.L. Shnyrov, Analysis of differential scanning calorimetry data for proteins. Criteria of validity of one-step mechanism of irreversible protein denaturation, Biophys. Chem. 69 (1997) 125–135.
[24] A.E. Lyubarev, B.I. Kurganov, A.A. Burlakova, V.N. Orlov, Irreversible thermal denaturation of uridine phosphorylase from Eschericia coli K-12, Biophys. Chem. 70 (1998) 247–257.
[25] L. Bao, S. Chatterjee, S. Lohmer, D. Schomburg, An irreversible and kinetically controlled process: thermal induced denaturation of L-2-hydroxyisocaproate dehydrogenase from Lactobacillus confuses, Protein J. 26 (2007) 143–151.
[26] D. Rodriguez-Larrea, S. Minning, T.V. Borchert, J.M. Sanchez-Ruiz, Role of solvation barriers in protein kinetic stability, J. Mol. Biol. 360 (2006) 715–724.
[27] R. Lumry, H. Eyring, Conformational changes of proteins, J. Phys. Chem. 58 (1954) 110–120.
[28] K. Idakieva, P. Nikolov, I. Chakarska, N. Genov, V.L. Shnyrov, Spectroscopic properties and conformational stability of Concholepas concholepas hemocyanin, J. Fluoresc. 18 (2008) 715–725.
[29] M. Weijers, P.A. Barneveld, M.A. Cohen Stuart, R.W. Visschers, Heat-induced denaturation and aggregation of ovalbumin at neutral pH described by irreversible first-order kinetics, Protein Sci. 12 (2003) 2693–2703.